Fibroblast growth factor receptor 3 mutation attenuates response to immune checkpoint blockade in metastatic urothelial carcinoma by driving immunosuppressive microenvironment

Yuxuan Song, Yun Peng, Caipeng Qin, Yulong Wang, Wenbo Yang, Yiqing Du, Tao Xu

Department of Urology, Peking University People's Hospital, Beijing, China

Correspondence to
Dr Tao Xu; xutao@pkuph.edu.cn

Dr Yiqing Du;
duyiqing@bjmu.edu.cn

ABSTRACT

Background Immune checkpoint blockade (ICB) therapy holds promise in metastatic urothelial carcinoma (UC). Fibroblast growth factor receptor 3 (FGFR3) mutation drives T-cell-depleted microenvironment in UC, which led to the hypothesis that FGFR3 mutation might attenuate response to ICB in patients with metastatic UC. The study aims to compare prognosis and response between patients with FGFR3-mutated and FGFR3-wildtype metastatic UC after ICB therapy, and decode the potential molecular mechanisms.

Methods Based on the single-arm, multicenter, phase 2 trial, IMvigor210, we conducted a propensity score matched (PSM) analysis. After a 1:1 ratio PSM method, 39 patients with FGFR3-mutated and 39 FGFR3-wildtype metastatic UC treated with atezolizumab were enrolled. A meta-analysis through systematical database retrieval was conducted for validation. In addition, we performed single-cell RNA sequencing on three FGFR3-mutated and three FGFR3-wildtype UC tumors and analyzed 58,069 single cells.

Results The PSM analysis indicated FGFR3-mutated patients had worse overall survival (OS) in comparison to FGFR3-wildtype patients (HR=2.11, 95% CI=(1.16 to 3.85), p=0.015) receiving atezolizumab. The median OS was 9.2 months (FGFR3-mutated) versus 21.0 months (FGFR3-wildtype). FGFR3-mutated patients had lower disease control rate than FGFR3-wildtype patients (41.0% vs 66.7%, p=0.023). The meta-analysis involving 938 patients with metastatic UC confirmed FGFR3 mutation was associated with worse OS after ICB (HR=1.28, 95% CI=(1.04 to 1.59), p=0.02). Single-cell RNA transcriptome analysis identified FGFR3-mutated UC carried a stronger immunosuppressive microenvironment compared with FGFR3-wildtype UC. FGFR3-mutated UC exhibited less immune infiltration, and lower T-cell cytotoxicity. Higher TREM2+ macrophage abundance in FGFR3-mutated UC can undermine and suppress the T cells, potentially contributing to the formation of an immunosuppressive microenvironment. Lower inflammatory-cancer-associated fibroblasts in FGFR3-mutated UC recruited

WHAT IS ALREADY KNOWN ON THIS TOPIC

⇒ Immune checkpoint blockade (ICB) therapy holds promise in metastatic urothelial carcinoma (UC) and fibroblast growth factor receptor 3 (FGFR3) mutation drives T-cell-depleted microenvironment in metastatic UC. But it is unknown whether FGFR3 mutation would attenuate pathological response and induce poor prognosis in patients with metastatic UC receiving ICB.

WHAT THIS STUDY ADDS

⇒ When treated with ICB, FGFR3-mutated patients had worse overall survival and lower disease control rate in comparison to FGFR3-wildtype patients.

⇒ Single-cell RNA transcriptome analysis identified FGFR3-mutated UC carries a stronger immunosuppressive microenvironment characterized by less immune cell infiltration, lower T-cell cytotoxicity, more immunosuppressive TREM2+ macrophages, and less inflammatory-cancer-associated fibroblasts in comparison with FGFR3-wildtype UC.

HOW THIS STUDY MIGHT AFFECT RESEARCH, PRACTICE OR POLICY

⇒ FGFR3 mutation can attenuate prognosis and pathological response to ICB in patients with metastatic UC.

⇒ FGFR3-mutated UC carries a stronger immunosuppressive microenvironment in comparison with FGFR3-wildtype UC.

⇒ Inhibition of FGFR3 might activate the immune microenvironment and the combination of FGFR inhibitor targeted therapy and ICB might be a promising therapeutic regimen in metastatic UC.

less chemokines in antitumor immunity but expressed growth factors to promote FGFR3-mutated malignant cell development. FGFR3-mutated UC carried abundance of malignant cells characterized by high hypoxia/metabolism and low interferon response phenotype.

Conclusions FGFR3 mutation can attenuate prognosis and response to ICB in patients with metastatic UC. FGFR3-mutated UC carries a stronger immunosuppressive microenvironment in comparison with FGFR3-wildtype UC. Inhibition of FGFR3 might activate the immune microenvironment, and the combination of FGFR inhibitor targeted therapy and ICB might be a promising therapeutic regimen in metastatic UC, providing important implications for UC clinical management.

INTRODUCTION

Immune checkpoint blockade (ICB) has been one of the most pivotal therapies in metastatic urothelial carcinoma (UC) treatment.[1 2] According to the most recent Society for Immunotherapy of Cancer guidelines and European Association of Urology guidelines on metastatic UC,[1 2] ICB has become first-line combination therapy with chemotherapy in patients fit for platinum-based treatment,[3–5] first-line immunotherapy in patients unfit for any platinum-based treatment,[6 7] and second-line immunotherapy for platinum pretreated patients.[8 9] Many efforts have explored the biomarkers used to predict response to ICB in metastatic UC. The US Food and Drug Administration (FDA) and the European Medicines Agency approved programmed death ligand 1 (PD-L1) expression as an indicator for first-line immunotherapy in patients unfit for cisplatin-based treatment and current evidence also confirmed the predictive value of PD-L1 in metastatic UC immunotherapy.[10] Tumor mutation burden (TMB) was also a vital biomarker approved by FDA[11] and randomized clinical trials validated that high TMB could help predict response to ICB in patients with UC.[12–14] Other biomarkers including molecular subtypes,[15 16] and CD8 expression[17 18] were also reported to be associated with response to ICB in preclinical studies or single-arm trials.

Fibroblast growth factor receptor 3 (FGFR3) is one of the high-frequency driver alterations in UC, ranging from 14% to 75%[15 16 19–21] in non-metastatic UC and from 11% to 24% in metastatic UC.[22–24] FGFR3 signaling is frequently activated by mutation and FGFR inhibitors as well as FGFR3 have been approved as a therapeutic target for UC by FDA.[25] In the past few years, many multiomics studies based on UC have identified a correlation between FGFR3 mutation and T-cell-depleted microenvironment.[21 26–28] The driving effects of FGFR3 alteration on the decreased T-cell infiltration in UC have been demonstrated in vitro, and FGFR3 inhibitor combined with ICB for effective CD8+T cell-mediated antitumor efficacy has been detected in vivo.[28 29] These data have further led to the hypothesis that patients with UC harboring FGFR3 mutation might have attenuated response and poor prognosis compared with patients without FGFR3 mutation when treated with ICB.

However, recent clinical trials[24 30 31] found that the response to ICB in patients with UC harboring FGFR3 mutation was similar to that in patients without FGFR3 mutation. The above-mentioned clinical evidence showed inconsistent results with multiomics studies. In addition, the current clinical studies are limited by (1) unbalanced and uncomparable baseline characteristics between FGFR3-mutated and FGFR3-wildtype patients, and (2) deficient sample size in each study to get convincing conclusions.

Therefore, we performed a propensity score matched (PSM) analysis and a systematic review and meta-analysis of available clinical evidence including trials and real-world studies to evaluate the predictive value of FGFR3 mutation in patients with metastatic UC treated with ICB. In addition, we also explored the potential mechanism for the effects of FGFR3 mutation on ICB through single-cell RNA sequencing.

METHODS

PSM analysis of IMvigor210 immunotherapy cohort

IMvigor210 study is a single-arm, multicenter, phase 2 trial investigating the ICB atezolizumab in patients with metastatic UC (NCT02951767 and NCT02108652).[12 18] Genomic data and clinical data for the IMvigor210 cohort were extracted from the R package IMvigor210CoreBiologies (http://research-pub.gene.com/IMvigor210CoreBiologies/). Genomic data were assessed according to publicly available data from the IMvigor210 study derived from hybrid capture-based next-generation sequencing-based genomic profiling (Foundation Medicine, Cambridge, Massachusetts, USA), as previously described.[18]

Clinicopathological and genomic data, including FGFR3 alternation status, sex, race, tobacco use history, intravesical Bacillus Calmette-Guérin (BCG) use, platinum-based chemotherapy use history, baseline Eastern Cooperative Oncology Group (ECOG) Performance Status Score, metastatic site, tissue sampling site for sequencing, TMB, PD-L1 tumor infiltrating immune cell (IC) status, survival status, survival time, and pathological response according to Response Evaluation Criteria In Solid Tumors V.1.1 were extracted. Only cases with complete data were included in subsequent analyses and cases with incomplete data were excluded.

The endpoints of interest were overall survival (OS) as the primary assessed outcome and pathological response of disease control rate as a secondary outcome. Disease control rate was defined as the rate of patients who achieved complete response, partial response, and stable disease. All analyses between FGFR3-mutated versus FGFR3-wildtype groups were first performed in all eligible metastatic UC cases. In order to reduce the biasing effect of potential confounders in our cohort, PSM with a 1:1 ratio was applied within the present cohort. Finally, 39 patients with FGFR3-mutated metastatic UC were matched with 39 of 168 patients with FGFR3-wildtype metastatic UC. Matching variables were as follows: sex, race, tobacco use history, intravesical BCG use, platinum-based chemotherapy use history, baseline ECOG Performance Status Score, metastatic site, tissue sampling site and TMB. Matching was performed using the optimal matching algorithm.[32] The driver oncogenic

mutation sites and non-driver mutation sites in FGFR3 were annotated and identified by OncoKB[33] (https://www.oncokb.org/).

Meta-analysis

We performed this study according to the Preferred Reporting Items for Systematic Reviews and Meta-Analyses guidelines.[34] We systematically searched PubMed, Embase, MEDLINE, Cochrane Library and ClinicalTrial.gov prior to December 1, 2022. Meeting abstracts from European Society of Medical Oncology and American Society of Clinical Oncology were also searched. Detailed search strategies were shown in online supplemental table 1. All investigations examined FGFR3 alternations and response to ICB in metastatic UC. Full details of literature search, inclusion and exclusion criteria, quality assessment of studies, and data extraction of meta-analysis are provided in online supplemental methods and materials.

Single-cell RNA sequencing and bioinformatic analysis

Three FGFR-mutated tumors and three FGFR3-wildtype tumors from six patients with UC were recruited in this study after approval by the Ethics Committee of Peking University People's Hospital. All patients in this study provided written informed consent for sample collection and data analyses. All enrolled samples were pathologically diagnosed with UC and the enrolled patients had no history of other cancers. The clinical characteristics of these patients are summarized in online supplemental table 2.

Full details of single-cell RNA sequencing bioinformatic analysis and validation of bulk RNA sequencing and microarray data analysis are provided in online supplemental methods and materials.

Statistical analysis

Median and interquartile range (IQR) were used to describe continuous data. Wilcoxon test was used to compare continuous data between two groups. Count and percentage were used to describe categorical data. X^2 test and Fisher's exact test were used to compare categorical data between two groups. Kaplan-Meier method, univariable, and multivariable Cox regression models were applied to perform prognostic survival analyses by calculating hazard ratio (HR) and 95% confidence interval (CI). Statistical analyses were performed by R software (V.4.1.2: http://www.r-project.org).

For meta-analysis, HR and 95% CI were used to compare time-to-event data and evaluate the relationships between survival outcomes and FGFR3 mutation. Risk ratio, risk difference (RD), and 95% CI were used to compare dichotomous variables and evaluate the relationships between pathological responses and FGFR3 mutation. Cochrane's Q test and Higgins I^2 statistic were used to measure the heterogeneity of enrolled studies. P value>0.05 of Cochrane's Q test and $I^2<50\%$ were considered as no detection of obvious heterogeneity and fixed-effect models were consequently used to calculate pooled results, otherwise random-effect models were used. Z-test was used to test statistical significance of pooled meta-analysis results. Sensitivity analysis measured the stability and robustness of pooled results using the leave-one-out method, by which the effect of each single study was evaluated through removing every single study and calculating the results every time. Begg's funnel plots were created to estimate the publication bias. All statistical analyses were carried out with ReviewManager V.5.3 (The Cochrane Collaboration) and Stata V.12.0 (Stata Corporation).

The two-sided p<0.05 was set as statistical significance.

RESULTS

IMvigor210 PSM cohort identified FGFR3-mutated UC exhibits worse prognosis and lower response to atezolizumab

The flowchart of patient selection in IMvigor210 PSM cohort is shown in figure 1.

Based on the inclusive and exclusive criteria, a total of 207 eligible patients with metastatic UC including 39 with FGFR3 mutation and 168 without FGFR3 mutation were enrolled from IMvigor210 cohort. The clinical characteristics of patients with metastatic UC with or without FGFR3 mutation are displayed in table 1. Before PSM, there was higher percentage of intravesical BCG use in FGFR3 mutation group than in FGFR3 wildtype group (41.0% vs 17.3%, p=0.002). For metastatic sites, FGFR3 mutation group had a higher proportion of patients with visceral metastasis and a lower proportion of patients with only lymph node metastasis than FGFR3 wildtype group (visceral metastasis: 69.2% vs 48.2%, only lymph node metastasis: 7.7% vs 20.8%, p=0.042).

After PSM, there were 39 pairs in FGFR3 mutation and matched FGFR3 wildtype groups. The clinical characteristics were all well balanced after PSM between the two groups (table 2). Since previous multiomics studies based on UC have reported FGFR3 mutation was enriched in T-cell-depleted tumors and the decreased T-cell-inflamed contexture might be driven by FGFR3 mutation,[26–28] the IMvigor210 cohort was used to explore the association between FGFR3 mutation and PD-L1 tumor infiltrating IC status. FGFR3 mutation group carried a lower proportion of IC1 and IC2+ than FGFR3 wildtype group (61.5% vs 79.2%, p=0.021; online supplemental table 3 and online supplemental figure 1), especially in IC2+ (42.3% vs 17.9%), which further confirmed the close relationship between FGFR3 mutation and immune-depletion in UC.

Before PSM, for the entire 39 FGFR3-mutated and 168 FGFR3-wildtype patients, there were no significant OS differences between FGFR3 mutation and FGFR3 wildtype groups (univariable Cox regression: HR=1.18, 95% CI=(0.76 to 1.82), p=0.455; figure 2A). The median OS was 9.2 months (IQR=5.9–not estimable (NE)) for FGFR3 mutation patients versus 11.1 months (IQR=9.0–15.4) for FGFR3 wildtype patients. In addition, FGFR3 mutation group had a similar disease control rate to FGFR3 wildtype group (41.0% vs 41.7%, p=0.942; figure 2B).
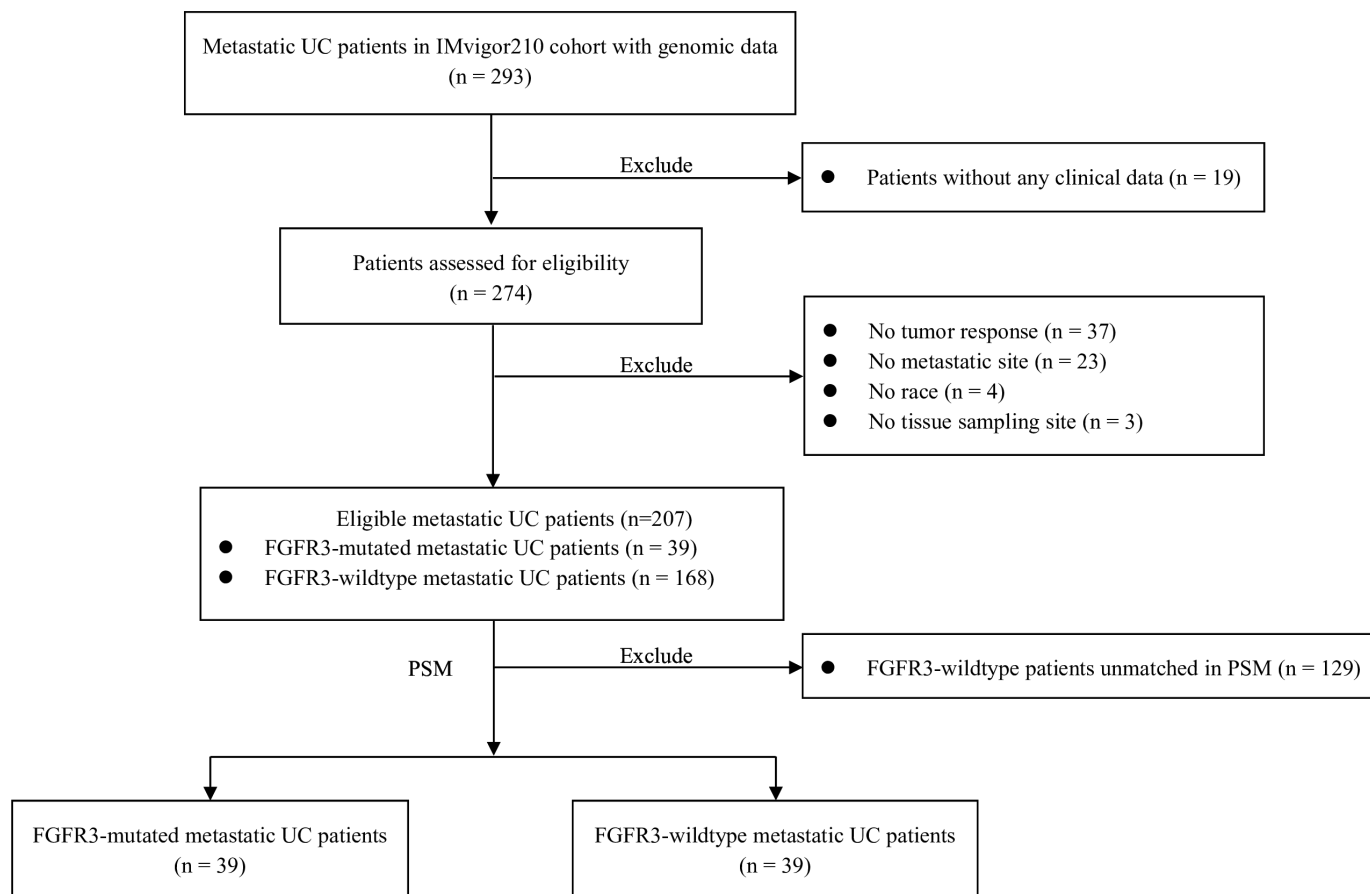
Figure 1 Flow diagram for the IMvigor210 immunotherapy cohort. A diagram depicting patients with metastatic UC included in the overall analysis (n=207) and PSM analysis (n=78). FGFR3, fibroblast growth factor receptor 3; PSM, propensity score matched; UC, urothelial carcinoma.

After PSM, for the matched 39 FGFR3-mutated and 39 FGFR3-wildtype patients, FGFR3 mutation group had worse OS in comparison to FGFR3 wildtype group (univariable Cox regression: HR=2.11, 95% CI=(1.16 to 3.85), p=0.015; figure 2C, table 3 and online supplemental table 4). The median OS was 9.2 months (IQR=5.9–NE) for FGFR3 mutation patients versus 21.0 months (IQR=13.3–NE) for FGFR3 wildtype patients. In addition, FGFR3 mutation group had a lower disease control rate than the FGFR3 wildtype group (41.0% vs 66.7%, p=0.023; figure 2D and table 3).

The multivariable Cox regression analyses were performed to further validate the effect of FGFR3 mutation on OS. The univariable Cox regression analyses (online supplemental table 4) identified that high TMB indicated a trend toward better OS (categorical data: HR=0.54, 95% CI=(0.27 to 1.07), p=0.079; continuous data: HR=0.97, 95% CI=(0.93 to 1.01), p=0.107), although the small sample size could not provide enough power to assess the effect and the statistical difference was not significant. Therefore, we used three multivariable Cox regression models to adjust the covariates: multivariable model 1 adjusted the TMB group (categorical data), multivariable model 2 adjusted TMB (continuous data), and multivariable model 3 adjusted PD-L1 tumor

infiltrating IC level (online supplemental table 5). The multivariable regression analyses indicated that FGFR3 mutation was independently associated with worse OS (model 1: HR=1.99, 95% CI=(1.08 to 3.64), p=0.026; model 2: HR=2.01, 95% CI=(1.10 to 3.68), p=0.023; model 3: HR=1.94, 95% CI=(1.06 to 3.56), p=0.032) after adjusting for TMB group, TMB, and PD-L1 tumor infiltrating IC level, respectively (online supplemental table 5).

We observed there were more TMB-high patients in FGFR3-wildtype group than FGFR3-mutated group (38.7% vs 28.2%, p=0.299), although not statistically significant in this small data set (table 1). The results suggested there might be potential relationships between TMB, FGFR3 mutation and OS. Therefore, we first evaluated TMB levels between patients with driver oncogenic FGFR3 mutations and patients with non-driver FGFR3 mutations in three immunotherapy cohorts (IMvigor210 cohort, Memorial Sloan Kettering Cancer Center (MSKCC) (metastatic bladder cancer (mBC)) cohort, and MSKCC (metastatic upper tract urothelial carcinoma (mUTUC) and metastatic urethral urothelial carcinoma (mUUC)) cohort) (online supplemental table 6). All FGFR3-mutated patients in IMvigor210 (n=39) and MSKCC (mUTUC and mUUC) (n=12)

Table 1 Baseline demographics in overall IMvigor210 cohort before PSM (n=207). Data were analyzed by χ^2 test and Wilcoxon test

Variables	FGFR3-mutated (n=39)	FGFR3-wildtype (n=168)	P value
Sex, n (%)			0.113
Female	12 (30.8)	30 (17.9)	
Male	27 (69.2)	138 (82.1)	
Race, n (%)			0.788
Non-white	3 (7.7)	18 (10.7)	
White	36 (92.3)	150 (89.3)	
Intravesical BCG use, n (%)			0.002
No	23 (59.0)	139 (82.7)	
Yes	16 (41.0)	29 (17.3)	
Platinum-based chemotherapy use history, n (%)			0.903
No	9 (23.1)	43 (25.6)	
Yes	30 (76.9)	125 (74.4)	
Metastatic site, n (%)			0.042
Lymph node only	3 (7.7)	35 (20.8)	
Liver	9 (23.1)	52 (31.0)	
Visceral*	27 (69.2)	81 (48.2)	
Baseline ECOG score, n (%)			0.659
0	17 (43.6)	66 (39.3)	
1	21 (53.8)	92 (54.8)	
2	1 (2.6)	10 (6.0)	
Tobacco, n (%)			0.579
Never	14 (35.9)	50 (29.8)	
Ever	25 (64.1)	118 (70.2)	
Tissue sampling site for sequencing, n (%)			0.453
Primary tumor tissue†	36 (92.3)	145 (86.3)	
Metasite tumor tissue‡	3 (7.7)	23 (13.7)	
PD-L1 tumor infiltrating IC level, n (%)			0.009
IC0	15 (38.5)	35 (20.8)	
IC1	17 (43.6)	62 (36.9)	
IC2+	7 (17.9)	71 (42.3)	
TMB (mut/MB), median (IQR)	7.2 (5.0–11.3)	7.7 (4.5–13.5)	0.472
TMB group, n (%)			0.299
High (≥10)	11 (28.2)	65 (38.7)	
Low (<10)	28 (71.8)	103 (61.3)	

*Visceral metastasis was defined as lung, bone, or any non-lymph node or soft tissue metastasis.
†Primary tumor tissue was from bladder, kidney, or ureter.
‡Metasite tumor tissue was from liver, lung, lymph node or other metastatic sites.
ECOG, Eastern Cooperative Oncology Group; FGFR3, fibroblast growth factor receptor 3 ; IC, immune cell; PD-L1, programmed death ligand 1; PSM, propensity score matched; TMB, tumor mutation burden.

carried driver oncogenic mutations in FGFR3. MSKCC (mBC) cohort contained 23 patients with driver oncogenic FGFR3 mutation and 6 patients with non-driver FGFR3 mutation. More than half (56.5–71.8%) of driver oncogenic FGFR3-mutated patients were TMB-low and carried a median TMB<10 mut/MB, whereas most (83.3%) of non-driver FGFR3-mutated patients were TMB-high and carried a median TMB of 14.1 mut/MB. In MSKCC (mBC) cohort, driver oncogenic FGFR3-mutated patients carried a trend toward lower TMB than non-driver FGFR3-mutated patients (median: 8.8 vs 14.1 mut/MB, Wilcoxon test p=0.374; TMB-high group

Table 2 Baseline demographics in IMvigor210 cohort after PSM (n=78). Data were analyzed by χ^2 test and Wilcoxon test

Variables	FGFR3-mutated (n=39)	FGFR3-wildtype (n=39)	P value
Sex, n (%)			0.437
Female	12 (30.8)	8 (20.5)	
Male	27 (69.2)	31 (79.5)	
Race, n (%)			0.239
Non-white	3 (7.7)	0 (0.0)	
White	36 (92.3)	39 (100.0)	
Intravesical BCG use, n (%)			1.000
No	23 (59.0)	22 (56.4)	
Yes	16 (41.0)	17 (43.6)	
Platinum-based chemotherapy use history, n (%)			1.000
No	9 (23.1)	10 (25.6)	
Yes	30 (76.9)	29 (74.4)	
Metastatic site, n (%)			0.881
Lymph node only	3 (7.7)	2 (5.1)	
Liver	9 (23.1)	10 (25.6)	
Visceral*	27 (69.2)	27 (69.2)	
Baseline ECOG score, n (%)			0.383
0	17 (43.6)	20 (51.3)	
1	21 (53.8)	16 (41.0)	
2	1 (2.6)	3 (7.7)	
Tobacco, n (%)			0.321
Never	14 (35.9)	9 (23.1)	
Ever	25 (64.1)	30 (76.9)	
Tissue sampling site for sequencing, n (%)			0.193
Primary tumor tissue†	36 (92.3)	31 (79.5)	
Metasite tumor tissue‡	3 (7.7)	8 (20.5)	
PD-L1 tumor infiltrating IC level, n (%)			0.122
IC0	15 (38.5)	10 (25.6)	
IC1	17 (43.6)	14 (35.9)	
IC2+	7 (17.9)	15 (38.5)	
TMB (mut/MB), median (IQR)	7.2 (5.0–11.3)	8.1 (5.0–14.9)	0.258
TMB group, n (%)			0.471
High (≥10)	11 (28.2)	15 (38.5)	
Low (<10)	28 (71.8)	24 (61.5)	

*Visceral metastasis was defined as lung, bone, or any non-lymph node or soft tissue metastasis.
†Primary tumor tissue was from bladder, kidney, or ureter.
‡Metasite tumor tissue was from liver, lung, lymph node or other metastatic sites.
ECOG, Eastern Cooperative Oncology Group; FGFR3, fibroblast growth factor receptor 3 ; IC, immune cell; PD-L1, programmed death ligand 1; PSM, propensity score matched; TMB, tumor mutation burden.

proportion: 43.5% vs 83.3%, Fisher's exact test p=0.169; online supplemental table 6 and online supplemental figure 2). In addition, we further compared the survival and response between TMB-high and TMB-low groups in patients with driver oncogenic FGFR3 mutations. In driver FGFR3-mutated patients from IMvigor210 and MSKCC (mBC) cohorts, TMB-high and TMB-low patients showed similar OS and similar disease control rate (p>0.05) (figure 2E–F and online supplemental figure 3). However, in driver FGFR3-mutated patients from MSKCC (mUTUC and mUUC) cohort, TMB-high group had better OS in comparison to TMB-low group (univariable Cox regression: HR=0.16, 95% CI=(0.03 to 0.96), p=0.039; figure 2G).
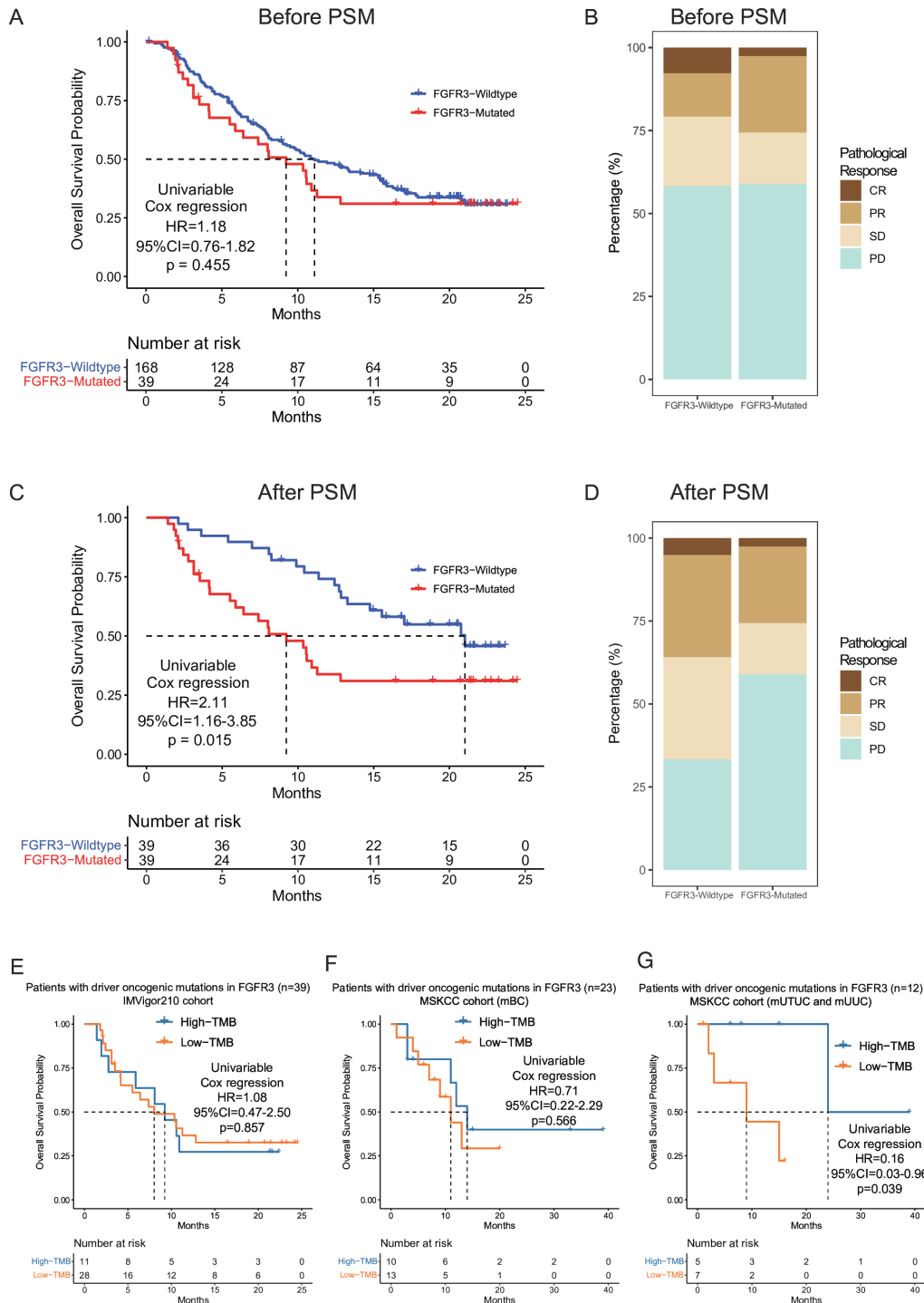
Figure 2 OS and pathological response in immunotherapy cohorts. Data were analyzed by univariable Cox regression model and χ² test. (A) Kaplan-Meier plot before PSM identified no significant OS differences (univariable Cox regression: HR=1.18, 95% CI=(0.76 to 1.82), p=0.455) between FGFR3-mutated (median OS=9.2 months, IQR=5.9–NE) and FGFR3-wildtype patients (median OS=11.1 months, IQR=9.0–15.4). (B) Disease control (CR+PR+SD) rate before PSM was similar between FGFR3-mutated and FGFR3-wildtype patients (41.0% vs 41.7%, p=0.942). (C) Kaplan-Meier plot after PSM identified worse OS (univariable Cox regression: HR=2.11, 95% CI=(1.16 to 3.85), p=0.015) in FGFR3-mutated (median OS=9.2 months, IQR=5.9–NE) than FGFR3-wildtype patients (median OS=21.0 months, IQR=13.3–NE). (D) Disease control rate after PSM was lower in FGFR3-mutated than FGFR3-wildtype patients (41.0% vs 66.7%, p=0.023). (E–G) Kaplan-Meier plot compared OS between high-TMB (≥10 mut/MB) and low-TMB (<10 mut/MB) groups in patients with driver FGFR3 oncogenic mutations based on IMvigor210 immunotherapy cohort, MSKCC (mBC) immunotherapy cohort, and MSKCC (mUTUC and mUUC) immunotherapy cohort. CR, complete response; FGFR3, fibroblast growth factor receptor 3; mBC, metastatic bladder cancer; MSKCC, Memorial Sloan Kettering Cancer Center; mUUC, metastatic urethral urothelial carcinoma; mUTUC, metastatic upper tract urothelial carcinoma; NE, not estimable; OS, overall survival; PD, progressive disease; PSM, propensity score matched; PR, partial response; SD, stable disease; TMB, tumor mutation burden.

Table 3 Comparison of prognosis and pathological response between FGFR3-mutated and FGFR3-wildtype patients in IMvigor210 cohort after PSM. Data were analyzed by χ^2 test

Variables	FGFR3-mutated (n=39)	FGFR3-wildtype (n=39)	P value
Median OS (months), median (IQR)	9.2 (5.9–NE)	21.0 (13.3–NE)	0.015
OS at 6 months, (%)	62.0	89.7	
OS at 1 year, (%)	33.8	74.1	
Tumor response, n (%)			0.136
CR	1 (2.6)	2 (5.1)	
PR	9 (23.0)	12 (30.8)	
SD	6 (15.4)	12 (30.8)	
PD	23 (59.0)	13 (33.3)	
Disease control rate (CR+PR+SD), n (%)	16 (41.0)	26 (66.7)	0.023

CR, complete response; FGFR3, fibroblast growth factor receptor 3 ; NE, not estimable; OS, overall survival; PD, progressive disease; PR, partial response; PSM, propensity score matched; SD, stable disease.

Meta-analysis revealed FGFR3 mutation attenuates survival and pathological response in metastatic UC receiving ICB

A total of 841 relevant studies were identified through initial search. After removing duplicates, 712 studies were left for further evaluation. After screening titles and abstracts, 14 studies were selected for full-text evaluation. According to the inclusive and exclusive criteria, six articles including eight retrospective cohort studies[24 31 35–38] were included into the final systematic review and meta-analysis (online supplemental figure 4).

The main characteristics of the included studies were detailed in table 4. The included eight retrospective cohort studies enrolled 938 patients with metastatic UC with FGFR3 mutation (n=169, 18.0%) or without FGFR3 mutation (n=769, 82.0%). Among the eight included studies, there was two single-arm clinical trials and six retrospective real-world studies. The two single-arm clinical trials (CheckMate275 and IMVigor210) used nivolumab and atezolizumab, respectively. And the other six retrospective real-world studies used multiple types of ICB. All the enrolled cohort studies were identified to be highly qualified by Newcastle-Ottawa Scale evaluation (online supplemental table 7).

Five articles[24 31 35 36 38] including seven studies reported data on the association between FGFR3 status and OS in patients with metastatic UC receiving ICB. Figure 3 revealed that FGFR3-mutated patients were significantly associated with worse OS than FGFR3-wildtype patients after ICB treatment (HR=1.28, 95% CI=(1.04 to 1.59), p=0.02). Two studies reported data on the association between FGFR3 status and progression-free survival (PFS) (online supplemental figure 5). Pooled results revealed that FGFR3 mutation was associated with worse PFS (HR=1.50, 95% CI=(1.06 to 2.12), p=0.02). Only one study reported FGFR3 status and disease specific survival, indicating FGFR3 status was not associated with disease specific survival (HR=5.42, 95% CI=(0.71 to 41.61), p=0.10).

Online supplemental figure 6 revealed that FGFR3-mutated patients were significantly associated with worse complete response rate than FGFR3-wildtype patients after ICB treatment (RD=−0.06, 95% CI=(−0.11 to −0.01), p=0.02). However, FGFR3 status was not associated with objective response rate and disease control rate (p>0.05) in patients with metastatic UC after ICB treatment.

Sensitivity analyses suggested no single study could influence the stability and robustness of pooled results through leave-one-out method (online supplemental figure 7). In addition, no evidence of publication bias existed through Begg's test (p=0.881) (online supplemental figure 8). The above results indicated the results of this meta-analysis proved to be firm.

FGFR3-mutated and FGFR3-wildtype tumors exhibits different tumor microenvironments

Bulk RNA sequencing expression data of 39 FGFR3-muated and 39 FGFR3-wildtype tumors in the IMvigor210 PSM cohort were analyzed for differential expressed genes. FGFR3-mutated tumors had lower expression of T-cell genes (CD3D, CD4, CD8A), cytotoxic effector genes (GZMA, IL-2RA), and terminal exhaustion genes (LAG3, PDCD1) than FGFR3-wildtype tumors (figure 4A). Upregulated genes of FGFR3-mutated tumors were mainly enriched in monocarboxylic acid and hormone metabolism, hypoxia, and stem cell functions. Upregulated genes of FGFR3-wildtype tumors were mainly enriched in leukocyte migration, immune response, and inflammatory response functions (figure 4A). IC analyses revealed FGFR3-mutated tumors had lower abundance of activated antitumor ICs (regulatory T cell (Treg), activated B cell, and mast cell) and higher abundance of immature dendritic cell and anaphylaxis-related ICs (type 2 T helper cell and eosinophil) (figure 4B).
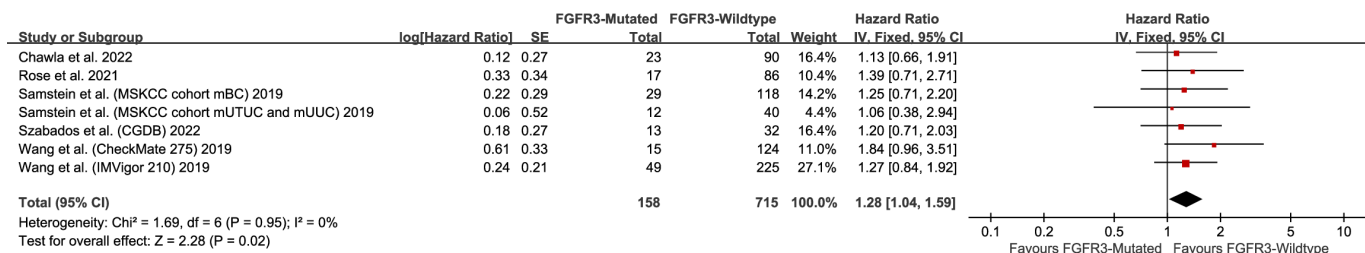
In order to further analyze the role of FGFR3 in UC, microarray data from RT-112 bladder cancer cell lines with or without short hairpin RNA knockdown of FGFR3 were

Table 4 Characteristics of included studies in systematic review and meta-analysis

First author	Trial name/cohort name	No. of patients with metastatic UC			Immune checkpoint blockade treatment	Median follow-up time (months)	Method for FGFR3 mutation	Survival outcomes (HR (95% CI))	Pathological responses	
		Year	FGFR3-mutated	FGFR3-wildtype					FGFR3-mutated	FGFR3-wildtype
Wang et al[24]	CheckMate275	2019	15	124	Nivo	7.0	DNA sequencing	OS: 1.84 (0.96 to 3.51)	CR: 1 PR: 2 SD: 1 PD: 10	CR: 9 PR: 17 SD: 27 PD: 51
Wang et al[24]	IMVigor210	2019	49	225	Atezo	11.7	DNA sequencing	OS: 1.27 (0.84 to 1.92)	CR: 1 PR: 11 SD: 7 PD: 25	CR: 20 PR: 28 SD: 37 PD: 108
Samstein et al[36]	MSKCC cohort (mBC)	2019	29	118	Atezo/Ave/Durva/Nivo/Pembro/Ipi/Treme	8.0	DNA sequencing	OS: 1.25 (0.71 to 2.20)	–	–
Samstein et al[36]	MSKCC cohort (mUTUC and mUUC)	2019	12	40	Atezo/Ave/Durva/Nivo/Pembro/Ipi/Treme	8.0	DNA sequencing	OS: 1.06 (0.38 to 2.94)	–	–
Szabados et al[35]	Clinico-Genomic Database	2022	13	32	Atezo/Durva/Nivo/Pembro	9.4	DNA sequencing	OS: 1.20 (0.71 to 2.03)	–	–
Rose et al[31]	–	2021	17	86	Atezo/Ave/Durva/Nivo/Pembro	8.8	DNA sequencing	OS: 1.39 (0.71 to 2.71) PFS: 1.46 (0.90 to 2.39)	CR: 1 PR: 1 SD: 2 PD: 13	CR: 7 PR: 9 SD: 9 PD: 61
Chawla et al[38]	–	2022	23	90	Atezo/Durva/Nivo/Pembro/Ipi/Treme/Sparta/Lerami	14.6	DNA sequencing	OS: 1.13 (0.66 to 1.91) PFS: 1.54 (0.94 to 2.51)	–	–
Tully et al[37]	–	2021	11	54	Nivo/Pembro/Atezo	7.8	RT-PCR	DSS: 5.42 (0.71 to 41.61)	–	–

Atezo, atezolizumab; Ave, avelumab; CR, complete response; DSS, disease specific survival; Durva, durvalumab; HR, hazard ratio; Ipi, ipilimumab; Lerami, leramilimab; mBC, metastatic bladder cancer; MSKCC, Memorial Sloan Kettering Cancer Center; mUTUC, metastatic upper tract urothelial carcinoma; mUUC, metastatic urethral urothelial carcinoma; Nivo, nivolumab; OS, overall survival; PD, progressive disease; Pembro, pembrolizumab; PFS, progression-free survival; PR, partial response; RT-PCR, reverse transcription-PCR; SD, stable disease; Sparta, spartalizumab; Treme, tremelimumab.

Study or Subgroup	log[Hazard Ratio]	SE	FGFR3-Mutated Total	FGFR3-Wildtype Total	Weight	Hazard Ratio IV. Fixed, 95% CI
Chawla et al. 2022	0.12	0.27	23	90	16.4%	1.13 [0.66, 1.91]
Rose et al. 2021	0.33	0.34	17	86	10.4%	1.39 [0.71, 2.71]
Samstein et al. (MSKCC cohort mBC) 2019	0.22	0.29	29	118	14.2%	1.25 [0.71, 2.20]
Samstein et al. (MSKCC cohort mUTUC and mUUC) 2019	0.06	0.52	12	40	4.4%	1.06 [0.38, 2.94]
Szabados et al. (CGDB) 2022	0.18	0.27	13	32	16.4%	1.20 [0.71, 2.03]
Wang et al. (CheckMate 275) 2019	0.61	0.33	15	124	11.0%	1.84 [0.96, 3.51]
Wang et al. (IMVigor 210) 2019	0.24	0.21	49	225	27.1%	1.27 [0.84, 1.92]
Total (95% CI)			**158**	**715**	**100.0%**	**1.28 [1.04, 1.59]**

Heterogeneity: Chi² = 1.69, df = 6 (P = 0.95); I² = 0%
Test for overall effect: Z = 2.28 (P = 0.02)

Figure 3 Forest plots showing patients with FGFR3-mutated metastatic urothelial carcinoma had worse overall survival than FGFR3-wildtype patients after immune checkpoint blockade treatment. FGFR3, fibroblast growth factor receptor 3; CGDB, Clinico-Genomic Database; mBC, metastatic bladder cancer; MSKCC, Memorial Sloan Kettering Cancer Center; mUUC, metastatic urethral urothelial carcinoma; mUTUC, metastatic upper tract urothelial carcinoma.

analyzed. Interferon response genes (BST2, TMEM140) and inflammatory response genes (IL-1R1, C3AR1) were upregulated in bladder cell lines with knockdown of FGFR3, while and metabolism-related genes (LDLR, IDI1, ACAT2) were downregulated (online supplemental figure 9). Gene set variation analysis (GSVA) and gene set enrichment analysis (GSEA) identified immune-related hallmarks were upregulated and metabolism-related hallmarks were downregulated in bladder cell lines with knockdown of FGFR3 (figure 4C–D).

Single-cell RNA sequencing identified FGFR3-mutated UC carries higher epithelial cells and lower ICs

To further decode the differences of tumor microenvironment between FGFR3-mutated and FGFR3-wildtype UC, we selected six UC tumors (three FGFR3-mutated and three FGFR3-wildtype) and performed droplet-based single-cell RNA sequencing (figure 5A). After quality control, a total of 58,069 single cells were enrolled for subsequent analysis (online supplemental figure 10A). Among these cells, 32,250 cells (55.5%) were from FGFR3-mutated tumors and 25,819 cells (44.5%) were from FGFR3-wildtype tumors. All qualified cells were clustered into seven major cell types with classic markers: epithelial cells (EPCAM$^+$), T/natural killer cells (CD3D$^+$CD3E$^+$CD3G$^+$ or NCAM1$^+$), myeloid cells (C1QA$^+$S100A8$^+$), B/plasma cells (CD79A$^+$), fibroblast cells (COL1A1$^+$), endothelial cells (VWF$^+$), and mast cells (TPSB2$^+$) (figure 5B–C and online supplemental figure 10B-C). The relative proportion of epithelial cells in FGFR3-mutated UC was higher than the FGFR3-wildtype UC (41.9% vs 4.3%, p<0.001). However, the proportions of ICs and stromal cells in FGFR3-mutated UC were lower than FGFR3-wildtype UC (p<0.001) (figure 5D–E, online supplemental figure 10C-E, and online supplemental table 8).

High hypoxia/metabolism-related hallmark and low immune-related signature in FGFR3-mutated malignant cells

Next, we extracted all the 14,611 epithelial cells and captured six patient-specific cell clusters (figure 6A). All FGFR3-mutated tumors had FGFR3 expression, while FGFR3-wildtype tumors rarely expressed FGFR3 (figure 6B). We inferred large-scale chromosomal copy number variations (CNVs) of all epithelial cells with

immune and stromal cells as references. All epithelial cells were malignant cells and the six clusters had patient-specific CNV patterns (figure 6C and online supplemental figure 11A). GSVA identified that malignant cells from FGFR3-mutated tumors upregulated hypoxia-related and metabolism-related pathways, whereas FGFR3-wildtype tumors upregulated immune response hallmarks (figure 6D). The hypoxia-related and metabolism-related scores and markers of FGFR3-mutated malignant cells were significantly higher than the FGFR3-wildtype group (p<0.001). The interferon response scores and markers of FGFR3-wildtype malignant cells were higher than the FGFR3-mutated group (p<0.001) (figure 6E–F). Since malignant cells were significantly enriched in FGFR3-mutated UC, we evaluated the above gene set score in predicting prognosis after ICB and found patients with higher oxidative phosphorylation score had worse OS and patients with higher interferon gamma response score had better OS in IMvigor210 immunotherapy cohort (figure 6G). We revealed the malignant cells in FGFR3-mutated UC demonstrated a higher hypoxia/metabolism-related state and a stronger immunosuppressive phenotype, which contributed to the poor prognosis and attenuated response in UC receiving ICB.

Lower T-cell cytotoxicity, more immunosuppressive TREM2+ macrophages, and lack of inflammatory-related fibroblast cells are identified in FGFR3-mutated tumor immune microenvironment

A total of 23,838 T and natural killer cells were clustered into eight subtypes: naive CD4+T cells (CD4$^+$CCR7$^+$), memory CD4+T cells (CD4$^+$IL-7R$^+$), CD4+Treg cells (CD4$^+$FOXP3$^+$), CD4+ exhausted cells (CD4$^+$TOX$^+$), effector CD8+T cells (CD8A$^+$GMZK$^+$), terminal exhausted cytotoxic CD8+T cells (CD8A$^+$LAG3$^+$), cycling T cells (MKI67$^+$), and natural killer cells (CD3D$^-$NCAM1$^+$) (figure 7A–B, online supplemental figure 11B-C, and online supplemental table 9). The relative proportions of all subtypes in FGFR3-mutated tumors were comparable to that in FGFR3-wildtype group (online supplemental figure 11C-D). The terminally exhausted score increased stepwise from naive to memory, Treg and exhausted CD4+T cells (online supplemental figure 12A-B). Developmental trajectory analysis of CD4+T cells identified
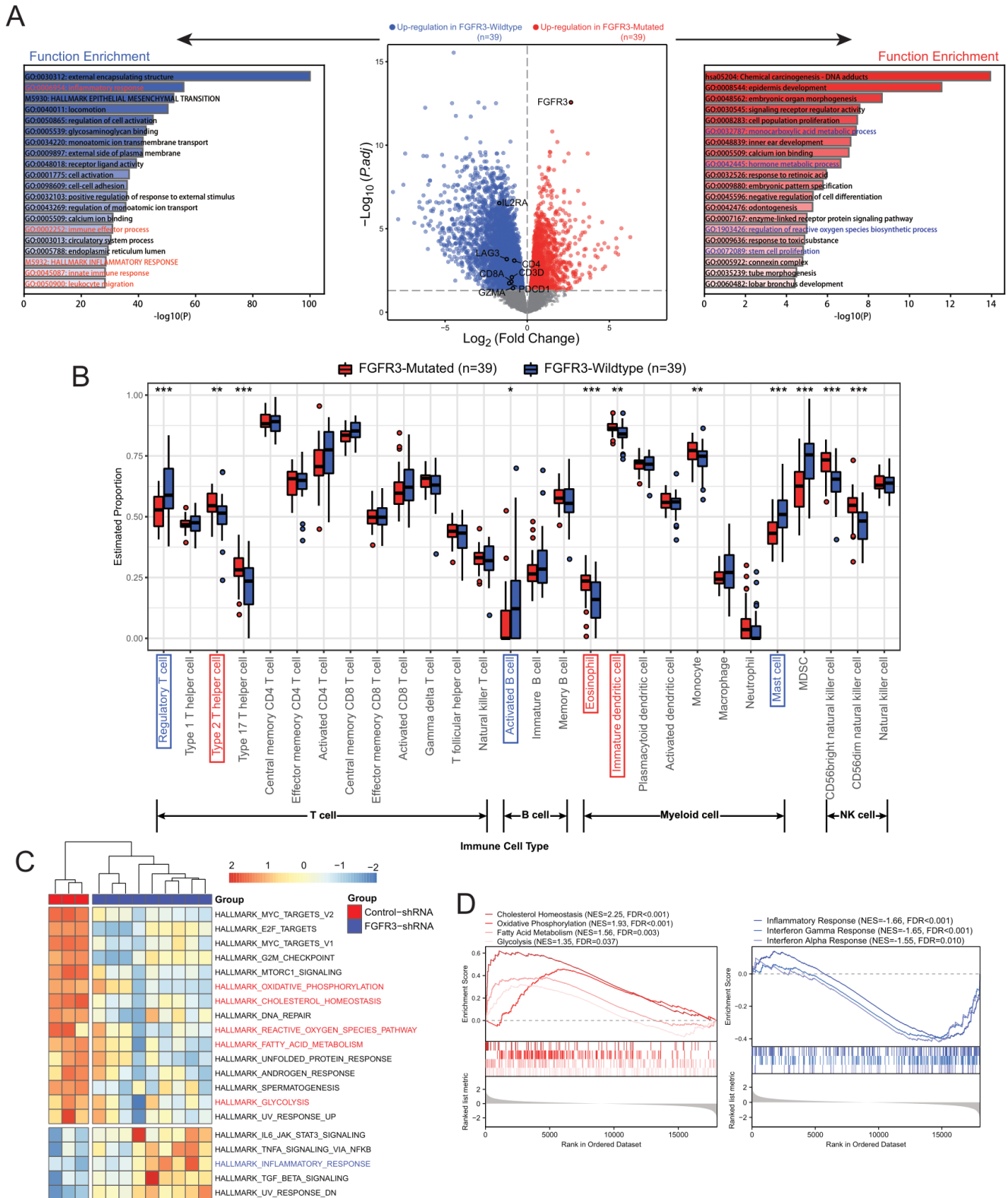
Figure 4 Bulk RNA sequencing and microarray data analysis indicated FGFR3-mutated and FGFR3-wildtype tumors shape different tumor microenvironments. (A) Bulk RNA sequencing expression data of 39 FGFR3-muated and 39 FGFR3-wildtype tumors in the IMvigor210 propensity score matched cohort found FGFR3-mutated UC had high hypoxia/metabolism features and FGFR3-wildtype UC carried high immune response. (B) Immune cell analyses revealed FGFR3-mutated tumors had lower abundance of activated antitumor immune cells. (C) Gene set variation analysis found immune-related hallmarks were upregulated and metabolism-related hallmarks were downregulated in bladder cell lines with knockdown of FGFR3. (D) Gene set enrichment analysis found metabolism-related pathways were upregulated and immune-related pathways were downregulated in bladder cell lines without knockdown of FGFR3. FDR, false discovery rate; FGFR3, fibroblast growth factor receptor 3; NES, normalized enrichment score; NK, natural killer; shRNA, short hairpin RNA; UC, urothelial carcinoma.
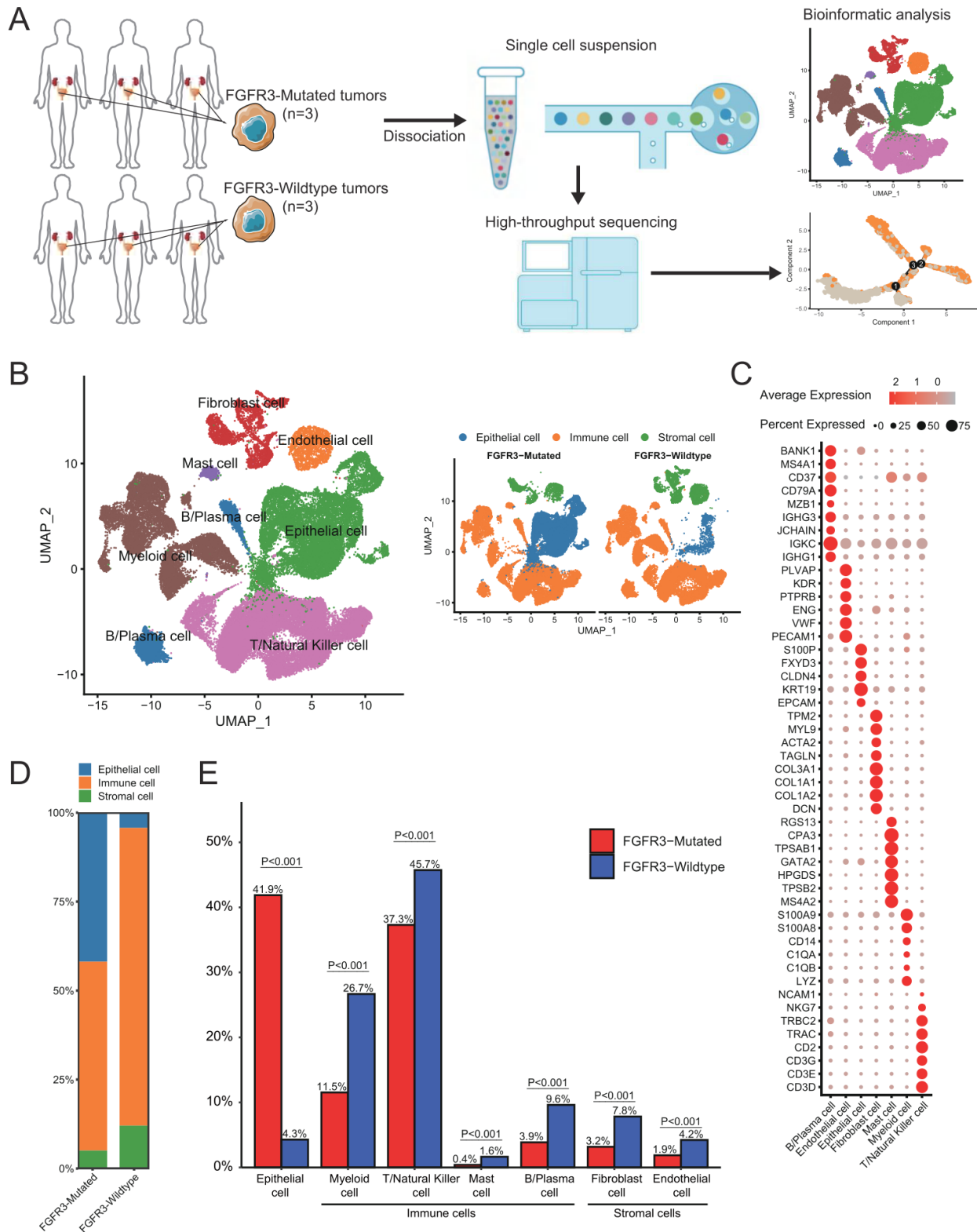
Figure 5 Single-cell RNA sequencing decoded FGFR3-mutated UC and FGFR3-wildtype UC. (A) Workflow diagram of the single-cell RNA sequencing analysis. (B) UMAP plot showed the major cell types in the UC ecosystem. (C) Dot plot showed the expression of marker genes in the major cell types. (D–E) Histogram showed the relative proportions of cells in FGFR3-mutated and FGFR3-wildtype tumors. FGFR3, fibroblast growth factor receptor 3; UC, urothelial carcinoma; UMAP, uniform manifold approximation and projection.

that naive CD4+T cells were the root, Treg and exhausted CD4+T cells were the end, and memory CD4+T cells were in a transitioning state (online supplemental figure

12C-D). Similar developmental trajectory analysis results were identified in CD8+T cells (online supplemental figure 12E-H). Effective and cytotoxic T cells in the
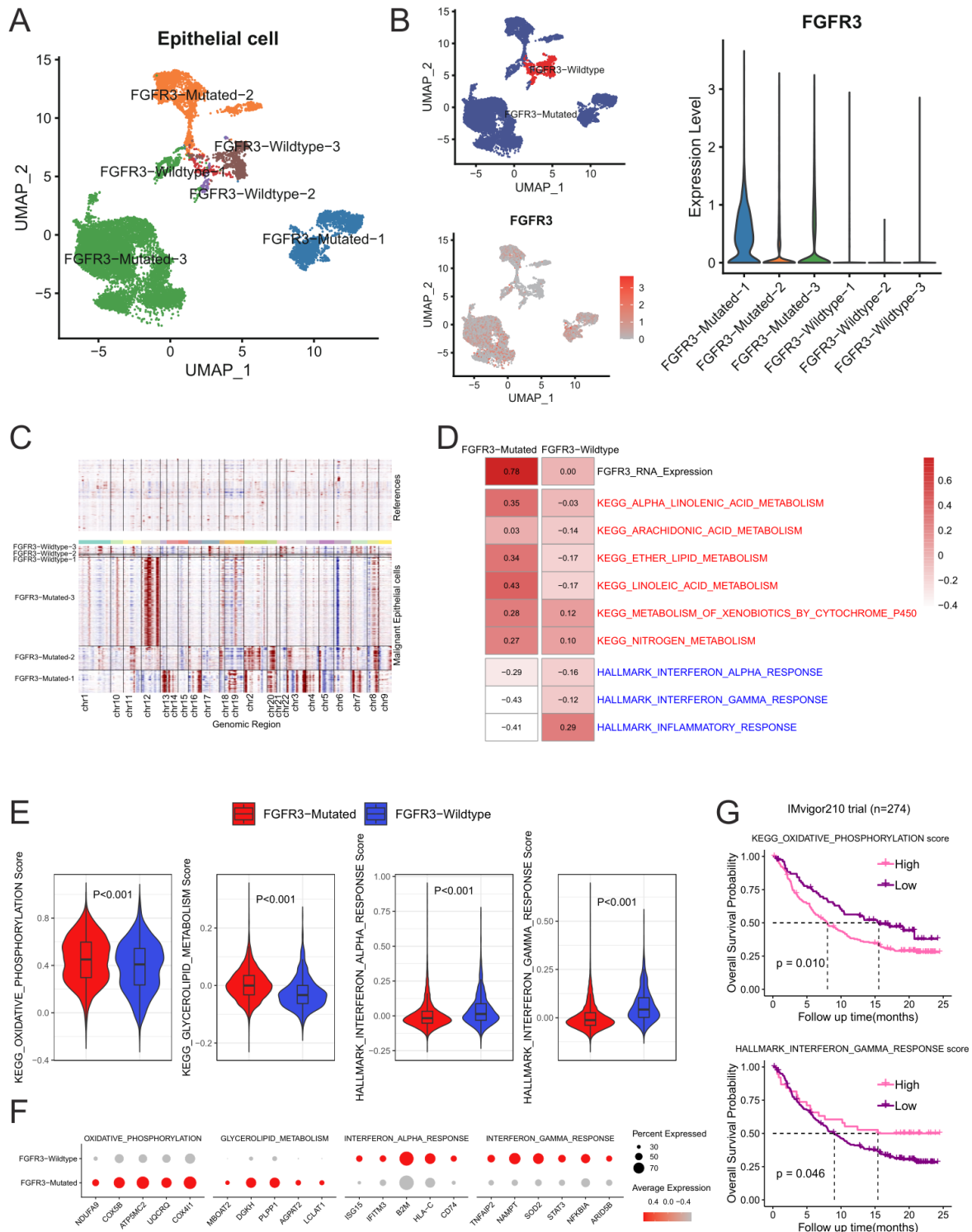
Figure 6 Single-cell RNA sequencing decoded the malignant epithelial cells between FGFR3-mutated UC and FGFR3-wildtype UC. (A) UMAP plot showed distinct patterns of malignant epithelial cells colored by each tumor sample. (B) UMAP plot and violin plot showed FGFR3 expression levels between FGFR3-mutated and FGFR3-wildtype malignant epithelial cells. (C) Heatmap showed large-scale copy number variations of single cells (rows) from five UC tumors. Red, amplifications; blue, deletions. (D) Gene set variation analysis of malignant cells in FGFR3-mutated and FGFR3-wildtype tumors compared hallmark signature from Molecular Signatures Database. (E) Violin plots showed hallmark scores of single cells between FGFR3-mutated and FGFR3-wildtype tumors. (F) Dot plot showed the expression levels of related markers of hallmarks in (E) between FGFR3-mutated and FGFR3-wildtype malignant cells. (G) Kaplan-Meier plot of bulk RNA sequencing identified patients with higher oxidative phosphorylation score had worse OS (univariable Cox regression: HR=1.58, 95% CI=(1.11 to 2.24), p=0.010) and patients with higher interferon gamma response score had better OS (univariable Cox regression: HR=1.23, 95% CI=(1.02 to 2.54), p=0.046) in IMvigor210 immunotherapy cohort. FGFR3, fibroblast growth factor receptor 3; OS, overall survival; UC, urothelial carcinoma; UMAP, uniform manifold approximation and projection.
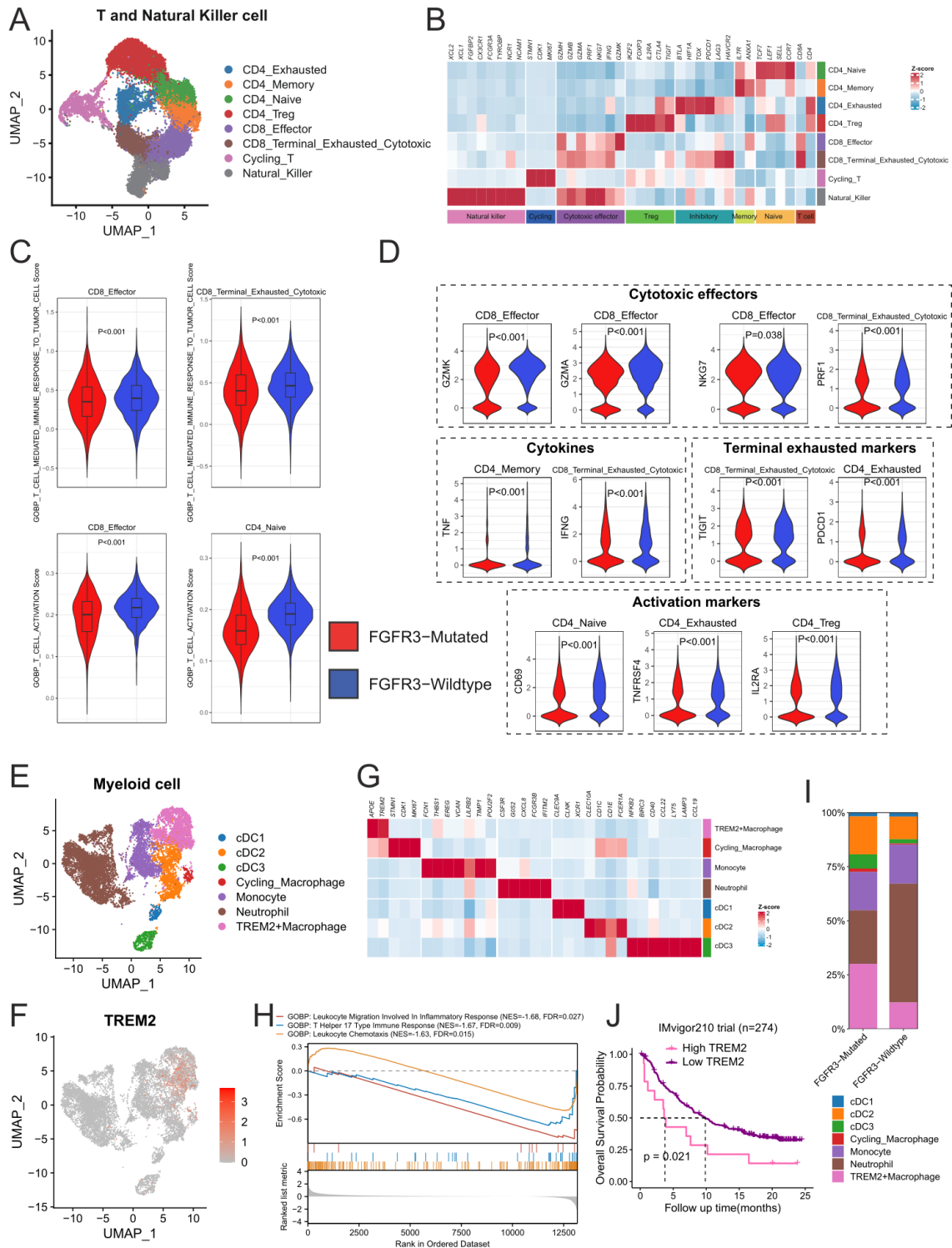
Figure 7 Single-cell RNA sequencing decoded the T and myeloid cells between FGFR3-mutated UC and FGFR3-wildtype UC. (A) UMAP plot showed the subtypes of T and natural killer cells. (B) Dot plot showed the expression of marker genes in cell subtypes. (C) Violin plots showed T-cell-related function scores of T cells between FGFR3-mutated and FGFR3-wildtype tumors. (D) Violin plots showed the expression levels of cytotoxic effectors, cytokines, terminal exhausted markers, and activation markers between FGFR3-mutated and FGFR3-wildtype T cells. (E) UMAP plot showed the subtypes of myeloid cells. (F) UMAP plot showed TREM2 expression in myeloid cells. (G) Heatmap showed the expression of marker genes in myeloid cell subtypes. (H) Gene set enrichment analysis identified TREM2+ macrophages downregulated the T-cell functions. (I) Histogram showed the relative proportions of myeloid cell subtypes between FGFR3-mutated and FGFR3-wildtype tumors. (J) Kaplan-Meier plot of bulk RNA sequencing identified higher TREM2 had worse overall survival (univariable Cox regression: HR=1.97, 95% CI=(1.10 to 3.55), p=0.021) in IMvigor210 immunotherapy cohort. cDC1, conventional type 1 dendritic cells; FDR, false discovery rate; FGFR3, fibroblast growth factor receptor 3; GOBP, gene ontology biological process; NES, normalized enrichment score; UC, urothelial carcinoma; UMAP, uniform manifold approximation and projection.

FGFR3-mutated group had lower scores of activation and immune response to tumors than those in FGFR3-wildtype group (p<0.001) (figure 7C). In addition, cytotoxic effectors, cytokines, terminal exhausted markers, and activation markers were significantly lower in FGFR3-mutated T cells compared with FGFR3-wildtype group (p<0.05) (figure 7D), which indicated T cells in FGFR3-wildtype UC were in a cytotoxic/exhausted state and T cells in FGFR3-mutated UC were in an unactivated state. Since cytotoxic T cells were the main focus of efforts to activate antitumor immunity and attack malignant cells,[18 39] the unactivated T-cell state in FGFR3-mutated UC might be the main factor to contribute to lower response and worse prognosis after ICB treatment.

A total of 10,606 myeloid cells were clustered into seven subtypes: macrophages (APOE[+]), monocytes (FCN1^{+}VCAN[+]), cycling macrophages (APOE[+]MKI67^{+}), neutrophils (CSF3R^{+}G0S2[+]), conventional type 1 dendritic cells (cDC1) (CLEC9A^{+}), cDC2 (CLEC10A^{+}), and cDC3 (LAMP3^{+}) (figure 7E–G, online supplemental figure 13A-B, and online supplemental table 10). Since most macrophages expressed high levels of TREM2, they were considered as TREM2+ macrophages (figure 7F). GSEA identified TREM2+ macrophages downregulated the T-cell immune response process (figure 7H), which was consistent with previous reports[40] that TREM2+ macrophages could undermine and suppress the T cells unleashed by ICB. The relative abundance of TREM2+ macrophages in the FGFR3-mutated group was significantly higher than that in FGFR3-wildtype group (30.1% vs 12.3%, p<0.001) (figure 7I). In addition, bulk RNA sequencing identified patients with higher TREM2 had worse OS in IMvigor210 immunotherapy cohort (figure 7J). Thus, these data suggested that the abundant TREM2+ macrophages in FGFR3-mutated tumors were more likely to undermine T cells and thus contributed to worse response to ICB, indicating TREM2 might be a treatment target in activating T cells and improving ICB.

A total of 3,043 fibroblast cells were clustered into two cancer-associated fibroblasts (CAFs): inflammatory-CAFs (iCAFs) (PDGFRA[+])[41] and myo-CAFs (RGS5^{+}) (figure 8A–C, online supplemental figure 13C, and online supplemental table 11). The iCAFs were associated with upregulation of inflammatory response, and IC chemotaxis and migration (figure 8D) and also exhibited strong expression of various cytokines and chemokines, such as CXCL1, CXCL6, CXCL12, and CXCL14 (figure 8B and online supplemental table 11). The relative abundance of iCAFs in the FGFR3-mutated group was significantly lower than that in FGFR3-wildtype group (44.0% vs 66.0%, p<0.001) (figure 8C), implying the lower abundance of iCAFs in FGFR3-mutated UC might recruit less ICs in antitumor immune response process.

Characterization of cell–cell interactions
To further explore the relationship among malignant cells, ICs, and stromal cells, we constructed the cell–cell interaction network among all cell types. Considering

the above-mentioned results, we first analyzed the ligand-receptor interaction pairs of cytokines between iCAFs and other immune or stromal cells (online supplemental figure 14A). Four pairs of cytokines (CXCL14_CXCR4, NR3C1_CXCL8, NR3C1_CCL2, and NR3C1_CCL11) were identified in all UC tumors. However, we found CXCL12_CXCR4, CXCL12_CXCR3 as well as CCR6_CCL20, CCR4_SLC7A1 were specifically identified in FGFR3-wildtype tumors, indicating FGFR3-mutated and FGFR3-wildtype tumors exhibited different patterns of cytokine activation in antitumor response.

FGFR3-mutated malignant epithelial cells expressed high levels of FGFR3 (figure 6B) and we then analyzed the ligand-receptor interaction pairs of growth factors between CAFs and malignant cells (online supplemental figure 14B). Interactions related to growth factor signaling, especially FGFR3-related interactions, were more abundant in FGFR3-mutated tumors in comparison to FGFR3-wildtype tumors, which suggested that the metabolism-related feature in FGFR3-mutated malignant cells might be owing to the active growth factor signaling.

In summary, single-cell RNA sequencing analysis revealed that FGFR3-mutated UC displayed more malignant cells with hypoxia/metabolism-related state and immunosuppressive phenotype, lower T-cell cytotoxicity, more immunosuppressive TREM2+ macrophages, and less inflammatory-related fibroblast cells in comparison to FGFR3-wildtype UC. The distinct patterns of tumor microenvironment between FGFR3-mutated versus FGFR3-wildtype tumors were displayed in figure 8E.

DISCUSSION
FGFR3 mutation was widely reported to be associated with UC prognosis, whereas it is still controversial. Patients with FGFR3-mutated UC usually have favorable prognosis and low histological grade,[42 43] whereas FGFR3 mutation could induce lower response and shorter time to recurrence in patients with locally advanced UC who received perioperative platinum-based chemotherapy.[44] Therefore, the role of FGFR3 mutation in UC prognosis is still controversial. Furthermore, the impact of FGFR3 mutation on prognosis and tumor response in patients with UC receiving immunotherapy remains inconclusive. We conducted a PSM analysis based on the immunotherapy cohort (IMvigor210) and further performed a systematic review and meta-analysis to evaluate the predictive value of FGFR3 mutation for response to ICB in patients with metastatic UC. This analysis brought out several meaningful findings.

First, IMvigor210 cohort illustrated FGFR3-mutated patients have significantly worse OS than FGFR3-wildtype patients after PSM. Subsequent meta-analysis confirmed the worse OS in patients with FGFR3-mutated metastatic UC through a larger sample size. Second, PSM analysis identified FGFR3-mutated patients have significantly lower disease control rate than FGFR3-wildtype patients,
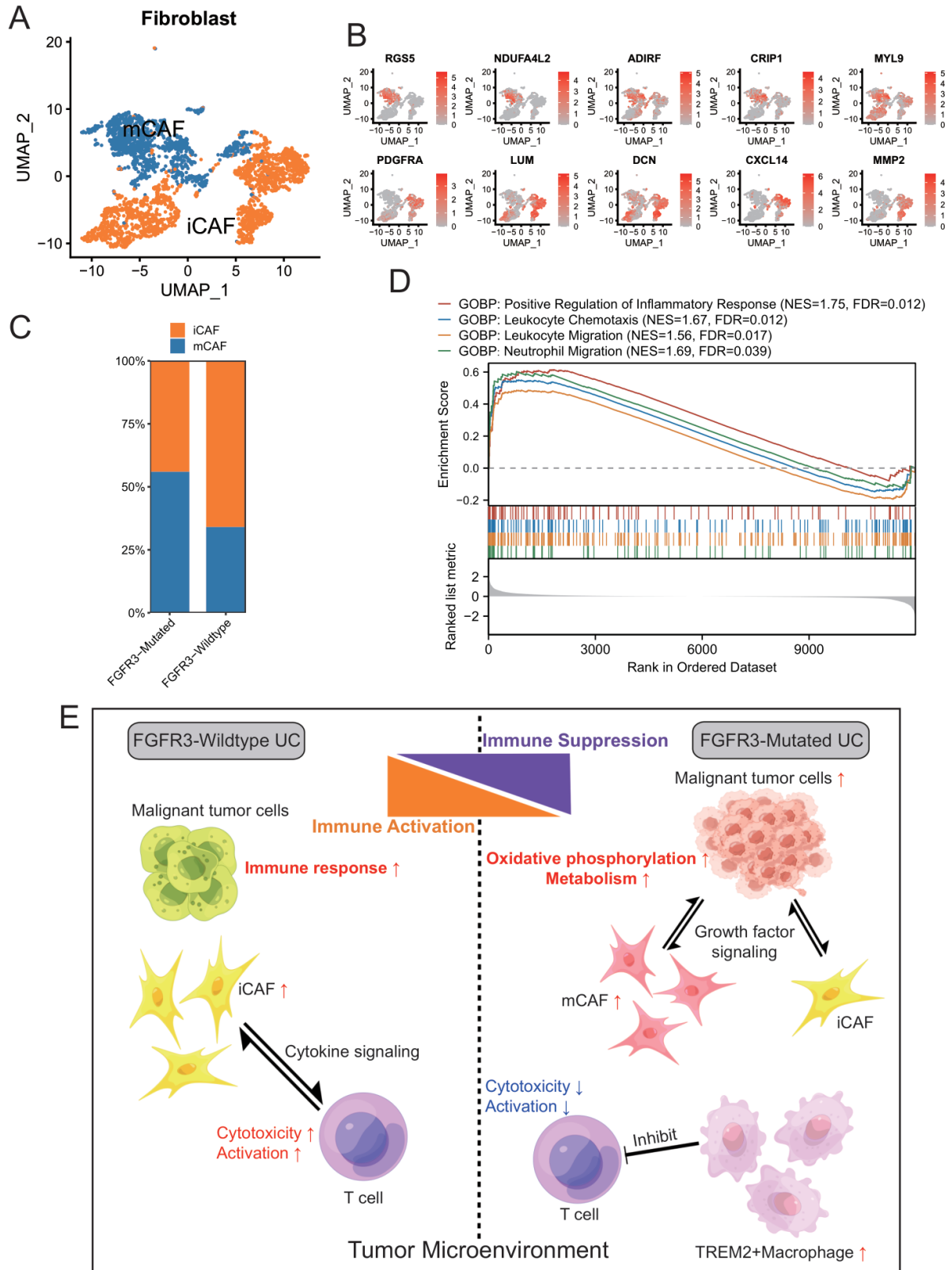
Figure 8 Single-cell RNA sequencing decoded the fibroblast cells and summary of tumor microenvironments between FGFR3-mutated and FGFR3-wildtype UC. UMAP plot showed the subtypes of fibroblast cells. (B) UMAP plots showed the expression of marker genes in fibroblast cell subtypes. (C) Histogram showed the relative proportions of fibroblast cell subtypes between FGFR3-mutated and FGFR3-wildtype tumors. (D) Gene set enrichment analysis identified iCAFs positively regulated immune response process. (E) Diagram summarized the distinct tumor microenvironments between FGFR3-mutated and FGFR3-wildtype UC. FDR, false discovery rate; FGFR3, fibroblast growth factor receptor 3; GOBP, gene ontology biological process; iCAF, inflammatory cancer-associated fibroblast; mCAF, myo-cancer-associated fibroblasts; NES, normalized enrichment score; UC, urothelial carcinoma; UMAP, uniform manifold approximation and projection.

indicating FGFR3 mutation would attenuate the response to ICB treatment.

Selection of an appropriate population of patients with metastatic UC to receive first-line or second-line immunotherapy is critical in metastatic UC clinical management. Most patients with metastatic UC received first-line or second-line treatment and less patients received third-line treatment, even though antibody-drug conjugates[45 46] and targeted therapies (FGFR inhibitors)[25 47] came into the novel agents for metastatic UC treatment. In addition, not all patients responded well to ICB[6 48] and 24.9% patients had immune-related adverse events.[49 50] Integration of the above-mentioned results from PSM analysis and meta-analysis suggests that FGFR3 mutation might be an indicator for predicting OS and ICB response. Patients with metastatic UC with FGFR3 mutation may be suboptimal candidates for ICB and FGFR3-wildtype patients may benefit more from ICB.

FGFR3 mutation has been acknowledged to be a predictive indicator for response to FGFR inhibitors[25] and immunotherapy has been approved for metastatic UC independently of FGFR3 mutation status. The present study was the first clinical analysis to propose FGFR3 mutation as a predictive factor for response to ICB. FGFR inhibitors and ICB could act synergistically and combined therapy might be a better option for the reason that FGFR inhibitors could elevate the effects of ICB through activating T cells.[29] Recently, the phase 2 NORSE study (NCT03473743)[51] demonstrated erdafitinib (FGFR inhibitor) plus cetrelimab (anti-programmed cell death 1 ICB) group appeared better overall response rate (68% vs 33%) and shorter time to response (1.8 months vs 2.3 months) than erdafitinib monotherapy group in patients with FGFR3-mutated metastatic UC, which proved the positive effects of combined therapy.

Our findings support the predictive value of FGFR3 mutation in metastatic UC treated with ICB for the first time through a PSM analysis and a meta-analysis. Wang *et al*[24] analyzed two immunotherapy clinical trials and found similar responses between FGFR3-mutated and FGFR3-wildtype UC groups. However, Wang *et al* did not balance the baseline characteristics, which could explain the statistically insignificant results.[24] In the present study, the baseline characteristics between the two groups were matched after PSM analysis of immunotherapy IMvigor210 cohort to mitigate the potential bias to some extent, which removed the impacts of confounding factors and made the two groups comparable. In addition, the sample size of patients with metastatic UC was further enlarged in meta-analysis through comprehensively retrieving databases and recruiting available data from clinical trials and real-world studies, which strengthened the stability of our findings.

TMB was a critical marker approved by FDA and many randomized clinical trials (KEYNOTE-010, KEYNOTE-045, and KEYNOTE-061) showed TMB-high patients could benefit more from pembrolizumab in comparison to chemotherapy.[11] The present study found that the patients with driver FGFR3 mutations usually had a trend toward lower TMB than non-driver FGFR3-mutated patients. In addition, we also observed an improved OS in TMB-high group than TMB-low group among driver FGFR3-mutated patients in one small size immunotherapy cohort, which implied the predictive value of combining TMB and FGFR3 status in immunotherapy.

Tumor microenvironment of UC contains tumor cells, T cells, myeloid cells, and stromal cells.[39 52 53] Interactions of various cell types in UC microenvironment play a vital role in tumor metastasis,[54] proliferation,[55] and immune evasion.[39] We used single-cell RNA sequencing to explore the tumor microenvironment and decode the potential mechanisms for the effects of FGFR3 mutation on ICB. FGFR3-mutated UC carries abundant malignant epithelial cells with high hypoxia/metabolism-related hallmark and strong immunosuppressive phenotype. In contrast, all types of ICs and stromal cells are at a lower level in FGFR3-mutated tumors compared with FGFR3-wildtype tumors. These data support the notion that FGFR3 mutation in UC drives an immune-depleted tumor microenvironment through attenuating the abundance of CD8+T cells and CD4+T cells, and interferon signaling.[28] Among the whole T-cell class, CD8+T cell infiltration is the core factor to shape the T-cell-inflamed microenvironment of UC[27] and cytotoxic CD8+T cells are considered as the main focus of efforts to perform antitumor immunity in various cancers.[52 56] We identified CD8+T cells in FGFR3-mutated tumors are in an unactivated state and carry lower cytotoxic functions, which might be used to explain the attenuated response to ICB treatment in FGFR3-mutated UC and support the phenomenon that FGFR3 inhibitor combined with ICB could rescue the attenuated CD8+T cell-mediated antitumor efficacy driven by FGFR3 mutation and further contribute to effective tumor suppression.[29] In addition, we observed that FGFR3-mutated tumors have higher abundance of TREM2+ macrophages, which might contribute to the lower cytotoxic state of T cells.[40] We also identified FGFR3-wildtype tumors carry higher iCAFs. However, iCAFs might be a double-edged sword: iCAFs might not only recruit chemokines to enhance the antitumor immune response but also express growth factors to promote FGFR3-mutated malignant cell development.

Despite the optimal matching algorithm of PSM analysis and comprehensive nature of systematic review were performed and single-cell RNA sequencing was conducted to decode the multicellular mechanisms, several preconditions and limitations of this study should still be taken into consideration. First, the sample size in IMvigor210 was small and it is difficult to detect some potential statistic difference, especially the relationships between TMB, FGFR3 mutation and prognosis. The limited sample size also could not provide enough power to evaluate these results to some extent. In order to eliminate the impact of the limited sample size as much as possible, we used two MSKCC cohorts for further validation and we verified the effect of FGFR3 mutation

through adjusting covariates in multivariate Cox models. Although we have made the above efforts, larger cohort studies are still required to facilitate this area. Second, this meta-analysis was based on the quality of reporting of the reviewed trials. Hence, some biases inherent to original studies might limit the validity of the findings. Third, the sample size of three FGFR3-mutated and three FGFR3-wildtype tumors for single cell analysis can hardly be representative to fully decode the differences between FGFR3-mutated and FGFR3-wildtype UC. It is necessary to further validate these findings in larger sample size studies. Fourth, with the current single-cell strategy, the spatial relationship of malignant cells and ICs could not be explored. Thus, spatial transcriptomics are required in future analyses to deeply investigate FGFR3-mutated UC.

CONCLUSIONS

In conclusion, our study found FGFR3 mutation can attenuate prognosis and response to ICB in patients with metastatic UC. FGFR3-mutated patients have worse OS and lower disease control rate than FGFR3-wildtype patients. FGFR3-mutated and FGFR3-wildtype tumors exhibit distinct features in the tumor microenvironment. FGFR3-mutated UC displays more malignant cells with hypoxia/metabolism-related state and immunosuppressive phenotype, and exhibited lower T-cell cytotoxicity, more immunosuppressive TREM2+ macrophages, and less iCAFs. Our findings suggest that FGFR3 could act as a biomarker to predict the therapeutic response to ICB in metastatic UC. Inhibition of FGFR3 might activate the immune microenvironment. FGFR inhibitor combined with ICB might elevate the effects of ICB through activating the T cells and overcoming ICB resistance in metastatic UC, which could contribute to guiding patients and clinicians when determining biomarker-driven personalized treatment strategies for metastatic UC.

cBioportal database (http://www.cbioportal.org/) Memorial Sloan Kettering Cancer Center immunotherapy cohort, and Gene Expression Omnibus database (accession numbers: GSE41035).

ORCID iD
Tao Xu http://orcid.org/0000-0003-3899-1500

REFERENCES

1. Cathomas R, Lorch A, Bruins HM, *et al*. The 2021 updated European Association of Urology guidelines on metastatic urothelial carcinoma. *Eur Urol* 2022;81:95–103.
2. Galsky MD, Balar AV, Black PC, *et al*. Society for Immunotherapy of cancer (SITC) clinical practice guideline on immunotherapy for the treatment of urothelial cancer. *J Immunother Cancer* 2021;9:e002552.
3. Powles T, Csőszi T, Özgüroğlu M, *et al*. Pembrolizumab alone or combined with chemotherapy versus chemotherapy as first-line therapy for advanced urothelial carcinoma (KEYNOTE-361): a randomised, open-label, phase 3 trial. *Lancet Oncol* 2021;22:931–45.
4. Powles T, van der Heijden MS, Castellano D, *et al*. Durvalumab alone and Durvalumab plus Tremelimumab versus chemotherapy in previously untreated patients with Unresectable, locally advanced or metastatic urothelial carcinoma (DANUBE): a randomised, open-label, multicentre, phase 3 trial. *Lancet Oncol* 2020;21:1574–88.
5. Galsky MD, Arija JÁA, Bamias A, *et al*. Atezolizumab with or without chemotherapy in metastatic urothelial cancer (IMvigor130): a multicentre, randomised, placebo-controlled phase 3 trial. *Lancet* 2020;395:1547–57.
6. Balar AV, Galsky MD, Rosenberg JE, *et al*. Atezolizumab as first-line treatment in cisplatin-ineligible patients with locally advanced and metastatic urothelial carcinoma: a single-arm, multicentre, phase 2 trial. *Lancet* 2017;389:67–76.
7. Balar AV, Castellano D, O'Donnell PH, *et al*. First-line Pembrolizumab in cisplatin-ineligible patients with locally advanced and unresectable or metastatic urothelial cancer (KEYNOTE-052): a multicentre, single-arm, phase 2 study. *Lancet Oncol* 2017;18:1483–92.
8. Bellmunt J, de Wit R, Vaughn DJ, *et al*. Pembrolizumab as second-line therapy for advanced urothelial carcinoma. *N Engl J Med* 2017;376:1015–26.
9. Powles T, Durán I, van der Heijden MS, *et al*. Atezolizumab versus chemotherapy in patients with platinum-treated locally advanced or metastatic urothelial carcinoma (IMvigor211): a multicentre. *The Lancet* 2018;391:748–57.
10. Davis AA, Patel VG. The role of PD-L1 expression as a predictive biomarker: an analysis of all US food and Drug Administration (FDA) approvals of immune checkpoint inhibitors. *J Immunother Cancer* 2019;7:278.
11. Marcus L, Fashoyin-Aje LA, Donoghue M, *et al*. FDA approval summary: pembrolizumab for the treatment of tumor mutational burden-high solid tumors. *Clin Cancer Res* 2021;27:4685–9.
12. Rosenberg JE, Hoffman-Censits J, Powles T, *et al*. Atezolizumab in patients with locally advanced and metastatic urothelial carcinoma who have progressed following treatment with platinum-based chemotherapy: a single-arm, Multicentre, phase 2 trial. *Lancet* 2016;387:1909–20.
13. Zheng M. Tumor mutation burden for predicting immune checkpoint blockade response: the more, the better. *J Immunother Cancer* 2022;10:e003087.
14. Bellmunt J, de Wit R, Fradet Y, *et al*. Putative biomarkers of clinical benefit with Pembrolizumab in advanced urothelial cancer: results

from the KEYNOTE-045 and KEYNOTE-052 landmark trials. *Clin Cancer Res* 2022;28:2050–60.

15 Kamoun A, de Reyniès A, Allory Y, *et al*. A consensus molecular classification of muscle-invasive bladder cancer. *Eur Urol* 2020;77:420–33.

16 Robertson AG, Kim J, Al-Ahmadie H, *et al*. Comprehensive molecular characterization of muscle-invasive bladder cancer. *Cell* 2017;171:540–56.

17 Szabados B, Kockx M, Assaf ZJ, *et al*. Final results of neoadjuvant atezolizumab in cisplatin-ineligible patients with muscle-invasive urothelial cancer of the bladder. *Eur Urol* 2022;82:212–22.

18 Mariathasan S, Turley SJ, Nickles D, *et al*. TGFβ attenuates tumour response to PD-L1 blockade by contributing to exclusion of T cells. *Nature* 2018;554:544–8.

19 Lindskrog SV, Prip F, Lamy P, *et al*. An integrated multi-Omics analysis identifies prognostic molecular subtypes of non-muscle-invasive bladder cancer. *Nat Commun* 2021;12:2301.

20 Moss TJ, Qi Y, Xi L, *et al*. Comprehensive genomic characterization of upper tract urothelial carcinoma. *Eur Urol* 2017;72:641–9.

21 Fujii Y, Sato Y, Suzuki H, *et al*. Molecular classification and diagnostics of upper urinary tract urothelial carcinoma. *Cancer Cell* 2021;39:793–809.

22 Damrauer JS, Beckabir W, Klomp J, *et al*. Collaborative study from the bladder cancer advocacy network for the genomic analysis of metastatic urothelial cancer. *Nat Commun* 2022;13:6658.

23 Nakauma-González JA, Rijnders M, van Riet J, *et al*. Comprehensive molecular characterization reveals genomic and transcriptomic subtypes of metastatic urothelial carcinoma. *Eur Urol* 2022;81:331–6.

24 Wang L, Gong Y, Saci A, *et al*. Fibroblast growth factor receptor 3 alterations and response to PD-1/PD-L1 blockade in patients with metastatic urothelial carcinoma. *Eur Urol* 2019;76:599–603.

25 Loriot Y, Necchi A, Park SH, *et al*. Erdafitinib in locally advanced or metastatic urothelial carcinoma. *N Engl J Med* 2019;381:338–48.

26 Su X, Lu X, Bazai SK, *et al*. Comprehensive integrative profiling of upper tract urothelial carcinomas. *Genome Biol* 2021;22:7.

27 Sweis RF, Spranger S, Bao R, *et al*. Molecular drivers of the non-T-cell-inflamed tumor microenvironment in urothelial bladder cancer. *Cancer Immunol Res* 2016;4:563–8.

28 Robinson BD, Vlachostergios PJ, Bhinder B, *et al*. Upper tract urothelial carcinoma has a luminal-papillary T-cell depleted contexture and activated FGFR3 signaling. *Nat Commun* 2019;10:2977.

29 Jing W, Wang G, Cui Z, *et al*. FGFR3 destabilizes PD-L1 via NEDD4 to control T-cell–mediated bladder cancer immune surveillance. *Cancer Res* 2022;82:114–29.

30 Necchi A, Raggi D, Giannatempo P, *et al*. Can patients with muscle-invasive bladder cancer and fibroblast growth factor Receptor-3 alterations still be considered for Neoadjuvant Pembrolizumab? A comprehensive assessment from the updated results of the PURE-01 study. *Eur Urol Oncol* 2021;4:1001–5.

31 Rose TL, Weir WH, Mayhew GM, *et al*. Fibroblast growth factor receptor 3 alterations and response to immune checkpoint inhibition in metastatic urothelial cancer: a real world experience. *Br J Cancer* 2021;125:1251–60.

32 Austin PC. A comparison of 12 algorithms for matching on the propensity score. *Stat Med* 2014;33:1057–69.

33 Chakravarty D, Gao J, Phillips SM, *et al*. OncoKB: a precision oncology knowledge base. *JCO Precis Oncol* 2017;2017.

34 Moher D, Liberati A, Tetzlaff J, *et al*. Preferred reporting items for systematic reviews and meta-analyses: the PRISMA statement. *BMJ* 2009;339:b2535.

35 Szabados B, Ponz-Sarvisé M, Machado R, *et al*. Clinico-Genomic characterization of patients with metastatic urothelial carcinoma in real-world practice identifies a novel bladder immune performance index. *Clin Cancer Res* 2022;28:4083–91.

36 Samstein RM, Lee C-H, Shoushtari AN, *et al*. Tumor mutational load predicts survival after immunotherapy across multiple cancer types. *Nat Genet* 2019;51:202–6.

37 Tully KH, Jütte H, Wirtz RM, *et al*. Prognostic role of FGFR alterations and FGFR mRNA expression in metastatic urothelial cancer undergoing checkpoint inhibitor therapy. *Urology* 2021;157:93–101.

38 Chawla NS, Sayegh N, Tripathi N, *et al*. Genomic and clinical prognostic factors in patients with advanced urothelial carcinoma receiving immune checkpoint inhibitors. *Clin Genitourin Cancer* 2023;21:69–75.

39 Oh DY, Kwek SS, Raju SS, *et al*. Intratumoral CD4⁺ T cells mediate anti-tumor cytotoxicity in human bladder cancer. *Cell* 2020;181:1612–25.

40 Molgora M, Esaulova E, Vermi W, *et al*. TREM2 modulation remodels the tumor myeloid landscape enhancing anti-PD-1 immunotherapy. *Cell* 2020;182:886–900.

41 Chen Z, Zhou L, Liu L, *et al*. Single-cell RNA sequencing highlights the role of inflammatory cancer-associated fibroblasts in bladder urothelial carcinoma. *Nat Commun* 2020;11:5077.

42 van Rhijn BWG, Mertens LS, Mayr R, *et al*. FGFR3 mutation status and FGFR3 expression in a large bladder cancer cohort treated by radical cystectomy: implications for anti-FGFR3 treatment? *Eur Urol* 2020;78:682–7.

43 van Oers JMM, Zwarthoff EC, Rehman I, *et al*. FGFR3 mutations indicate better survival in invasive upper urinary tract and bladder tumours. *Eur Urol* 2009;55:650–7.

44 Teo MY, Mota JM, Whiting KA, *et al*. Fibroblast growth factor receptor 3 alteration status is associated with differential sensitivity to platinum-based chemotherapy in locally advanced and metastatic urothelial carcinoma. *Eur Urol* 2020;78:907–15.

45 McGregor B, O'Donnell PH, Balar A, *et al*. Health-related quality of life of patients with locally advanced or metastatic urothelial cancer treated with enfortumab Vedotin after platinum and PD-1/PD-L1 inhibitor therapy: results from cohort 1 of the phase 2 EV-201 clinical trial. *Eur Urol* 2022;81:515–22.

46 Rosenberg JE, O'Donnell PH, Balar AV, *et al*. Pivotal trial of enfortumab Vedotin in urothelial carcinoma after platinum and anti-programmed death 1/programmed death ligand 1 therapy. *JCO* 2019;37:2592–600.

47 Lyou Y, Grivas P, Rosenberg JE, *et al*. Hyperphosphatemia secondary to the selective fibroblast growth factor receptor 1-3 inhibitor Infigratinib (BGJ398) is associated with antitumor efficacy in fibroblast growth factor receptor 3-altered advanced/metastatic urothelial carcinoma. *Eur Urol* 2020;78:916–24.

48 Siddiqui BA, Gheeya JS, Goswamy R, *et al*. Durable responses in patients with genitourinary cancers following immune checkpoint therapy rechallenge after moderate-to-severe immune-related adverse events. *J Immunother Cancer* 2021;9:e002850.

49 Wu Z, Chen Q, Qu L, *et al*. Adverse events of immune checkpoint inhibitors therapy for urologic cancer patients in clinical trials: a collaborative systematic review and meta-analysis. *Eur Urol* 2022;81:414–25.

50 Kawai T, Taguchi S, Nakagawa T, *et al*. Impact of immune-related adverse events on the therapeutic efficacy of pembrolizumab in urothelial carcinoma: a multicenter retrospective study using time-dependent analysis. *J Immunother Cancer* 2022;10:e003965.

51 Powles TB, Chistyakov V, Beliakouski V, *et al*. LBA27 Erdafitinib (ERDA) or ERDA plus Cetrelimab (CET) for patients with metastatic or locally advanced urothelial carcinoma (mUC) and fibroblast growth factor receptor alterations. *Ann Oncol* 2021;32:S1303.

52 van der Leun AM, Thommen DS, Schumacher TN. CD8+ T cell States in human cancer: insights from single-cell analysis. *Nat Rev Cancer* 2020;20:218–32.

53 Zhang Q, Liu S, Wang H, *et al*. ETV4 mediated tumor-associated neutrophil infiltration facilitates lymphangiogenesis and lymphatic metastasis of bladder cancer. *Adv Sci (Weinh)* 2023;10:2205613.

54 Huang M, Dong W, Xie R, *et al*. HSF1 facilitates the multistep process of lymphatic metastasis in bladder cancer via a novel PRMT5-WDR5-Dependent transcriptional program. *Cancer Commun (Lond)* 2022;42:447–70.

55 Zhang J, Zhou Q, Xie K, *et al*. Targeting WD repeat domain 5 enhances chemosensitivity and inhibits proliferation and programmed death-ligand 1 expression in bladder cancer. *J Exp Clin Cancer Res* 2021;40:203.

56 Tumeh PC, Harview CL, Yearley JH, *et al*. PD-1 blockade induces responses by inhibiting adaptive immune resistance. *Nature* 2014;515:568–71.